Characterizing the Influence of Human Presence on bistatic passive RFID-System

Dominik Lieckfeldt   Jiaxi You   Dirk Timmermann
Institute of Applied Microelectronics and Computer Engineering
University of Rostock
18119 Rostock, Germany
Email: {firstname.lastname}@uni-rostock.de

Abstract—Using simple and cost-effective tags, passive RFID systems offer a promising aid for identifying and localizing objects and users in indoor environments. Although systems based on radio frequencies usually suffer from multi-path interference and signal scattering, we show that the characteristics of such interference and scattering can be analyzed with passive RFID.

We present and analyze measurements of received signal strength (RSS) conducted in an indoor environment using a passive bistatic RFID-System. In order to characterize the influence of human presence on RSS, measurements were conducted for different user locations and orientations in an indoor deployment area.

Finally, an analytical approximation of the relation between user location and RSS is presented in accordance to our measurement results.

I. INTRODUCTION

Ubiquitous computing is one of the technological advances that will probably influence everyday life as devices are connected and, therefore, capable of communicating with each other. Ubiquitous systems typically contain sensors, actuators and communication modules that enable the subcomponents to exchange information in order to achieve a cooperative system that is more valuable than the sum of its components.

Typical inputs of such a system are location and identity of the ensemble members such as devices and users. It has been noted that Radio Frequency Identification (RFID) can facilitate acquiring such parameters and attracted considerable research effort. Passive RFID, as will be explained in more detail later, has the advantage of utilizing very small tags that can be attached to a multitude of different object types. These tags can communicate their unique identity number wireless and thereby facilitate identification.

Due to the complexity of RF-propagation, communication in such systems is a challenging task. Especially in indoor environments, fixtures, fittings and also humans can cause reflections, diffractions and absorptions of radio signals. Therefore, some commercial products use specialized hardware and try to increase accuracy by fusing several different metrics, like angle and range measurements. Since passive RFID-tags are powered by impinging radio energy only, they are especially sensitive to the impairing propagation effects. However, we show that the characteristics of the aforementioned adversary effects can be analyzed with a passive RFID system.

As a first step, we present detailed measurements of received signal strength (RSS) conducted in an indoor environment with a passive bistatic RFID system and focus on the impact of human presence near the communicating entities.

As we will show in the following, the spatial correlation of RSS fluctuations due to human presence, which are normally understood as impairment of wireless communication, can be analyzed with the our system. We consider the specific architecture of bistatic RFID-systems and quantify the significance of forward and reverse channels for this analyzis. Finally, we present analytical approximations to the measured relations which can be used to further study these effects through simulations. We also point out possible applications of the results presented.

II. RELATED WORK

Due to the significant influence of path loss, fading and interference on RFID systems, many works focus on characterizing these parameters. In [1] path loss and small-scale fading characteristics are measured in a bistatic RFID-system. The authors present cumulative density functions to approximate their observations and report that the path loss exponent of backscatter systems in indoor environments is approximately twice that of a single link system.

However, there are only a few works that consider the impact of human presence on received signal strength and its utility for localization. In [2], the authors consider the average absolute value of path loss difference on the wireless links of an indoor sensor network. Thereby, the passing of humans can be detected by the ceiling mounted senors and measurements can be combined to localize the human with an error of approximately 3 meters at 95% confidence level.

In [3], the authors' model for RF shadowing naturally represents the causes for changes of received signal strength as peaks (positive and negative) of a spatial loss field. The authors also apply this model to the localization of a person using a sensor network.

To the best of our knowledge, this work represents the first step towards a characterization of human induced RF-shadowing in bistatic RFID systems.

The remainder of the paper is organized as follows: Section III presents the architecture of the RFID-system used for the measurements and reviews a generic path loss model.
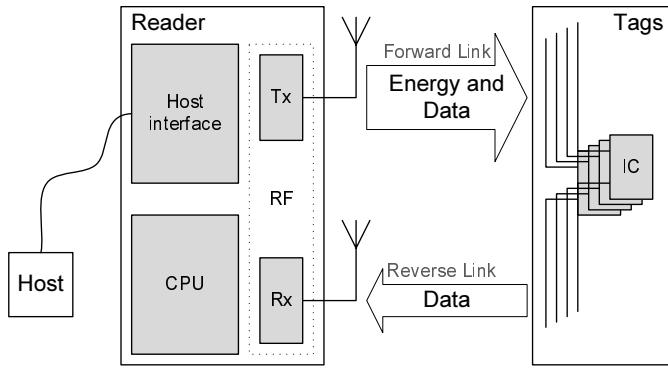
Figure 1. Architecture of bistatic RFID system.

In Section IV, we focus on the experimental set up and the measurement procedure. Section V gives information on the theoretical model of the influence of human presence on RSS. Furthermore, the measurements are analyzed and an approximations to the theoretical model are presented. Finally, we describe future research directions and conclude in Sections VI and VII.

III. ARCHITECTURE OF PASSIVE UHF RFID-SYSTEMS

In general, RFID systems consist of at least one so called *reader* device and typically many tags. Connected to the reader is typically a host computer which further processes the data from the tags. The reader contains a transceiver module and a processor to perform and coordinate communications between tags and host.

Passive backscatter RFID-systems can be divided into monostatic and bistatic systems depending upon whether receiving and transmitting is carried out by one or two independent antennas. Since transmit (A_{tx}) and receive (A_{rx}) antennas are separated physically in bistatic systems, the weaker receive signals from the tags do not need to be separated from the transmit signal by a coupler or circulator like in monostatic systems. Hence, the signal to noise ratio is improved which results in a potentially increased range of such systems. However, bistatic systems need more antennas which make them less applicable in situation where the space requirements are critical.

In bistatic systems it is important to distinguish between the forward link (A_{tx}-to-tag) and the backward link (tag-to-A_{rx}). Whereas the energy emitted by A_{tx} on the forward link powers the passive tags, the backward link is solely used for communicating the tag data to A_{rx} (figure 1). Such systems are forward link limited, meaning that impairments of the forward link greatly affect the readability of tags [4]. This stems from the minimum energy required by the tag IC for operations which is usually much larger than the reader sensitivity.

Commercial bistatic RFID systems usually provide several antenna ports and allow operating on arbitrary pairs of antennas for transmitting and receiving. The radio signals on each link are subject to propagation effects like fading and noise

which affect the signal strength. The next section reviews the path loss model of bistatic RFID systems.

A. Average Path Loss Model

The average path loss model describes the average attenuation of the transmit signal on forward and backward links. Let the reader's transmit power be $\mathcal{P}_{\text{t}}$ and the received power from tag i be $\mathcal{P}_{\text{i}}$. Considering the ideal free-space situation, the large-scale path loss of a bistatic RFID-System in dB is [1]:

$$\frac{\mathcal{P}_i}{\mathcal{P}_{\text{t}}} = G_{\text{tx},i}G_{\text{rx},i}(g_{\text{tx},i}\Gamma g_{\text{rx},i})\Omega \left(\frac{\lambda}{4\pi}\right)^4 \left(\frac{1}{d_{\text{tx},i}d_{\text{rx},i}}\right)^n \quad (1)$$

where $G_{\text{tx},i}$, $G_{\text{rx},i}$ are the gains of A_{tx} and A_{rx} and $g_{\text{tx},i}$, $g_{\text{rx},i}$ are the antenna gains of the i-th tag toward the receive and transmit antenna respectively. The parameters Ω and Γ are additional losses due to modulation and backscattering at the tag and n denotes the path-loss exponent.

In contrast to the ideal free-space model, the presence of obstacles near the line of sight (LOS) of forward and/or reverse channel typically influences average path loss. Therefore, we extend (1) to account for this effect and reformulate in dB:

$$P_i = P_{\text{t}} - L_{\text{p},i} \quad (2)$$
$$L_{\text{p},i} = L_0 + 10N \log_{10}(D_i) + L_{\text{obst},i} + L_{\text{other}} - L_{\text{g},i} \quad (3)$$

In a bistatic RFID system, the path loss is linear to $\sqrt{d_{\text{tx},i}d_{\text{rx},i}}$ [1]. Therefore, we use $D_i = \sqrt{d_{\text{tx},i}d_{\text{rx},i}}$ to characterize distances. Furthermore, $L_0 = -10 \log_{10} P_0$ and P_0 is the normalized received power at a distance D_0. $N = 2\,n$ denotes the total path loss exponent. $L_{\text{g},i}$ corresponds to the antenna gains and L_{other} accounts for losses Γ and Ω. $L_{\text{obst},i}$ represents the additional loss due to obstacles near the receiving and transmitting antenna or the tag and, therefore, depends on the position of the obstacle.

IV. CHARACTERIZATION OF MEASUREMENTS

This section describes the set-up of devices and parameters of the measurements.

A. Experimental Set-Up

We used the ALR-8800 RFID-reader from Alientechnology operating on ISM 868 MHz frequency band. Two circular polarized ($G = 5.5$ dB) and two linearly polarized ($G = 6$ dB) antennas are connected to its ports. All positions are relative to a coordinate system with its origin as depicted in figure 2. 69 passive RFID tags were deployed on the ground in a regular grid forming a quadratic area of side length $3.6\,m$. The four antennas were situated near the the edges of the deployment area at a height of $1.80\,m$ whereby antennas of the same type were at opposite edges. The set-up was situated in the middle of a $8.15\,m \times 6m$ room. To reduce the impact of reflection from adjacent walls, we paid attention that the antennas' main beam impinged in an acute angle which effectively caused all wall reflections to pass at least two walls before entering the deployment area.

The host computer was situated approximately 5 meter from the center of the deployment area. On the host computer ran a
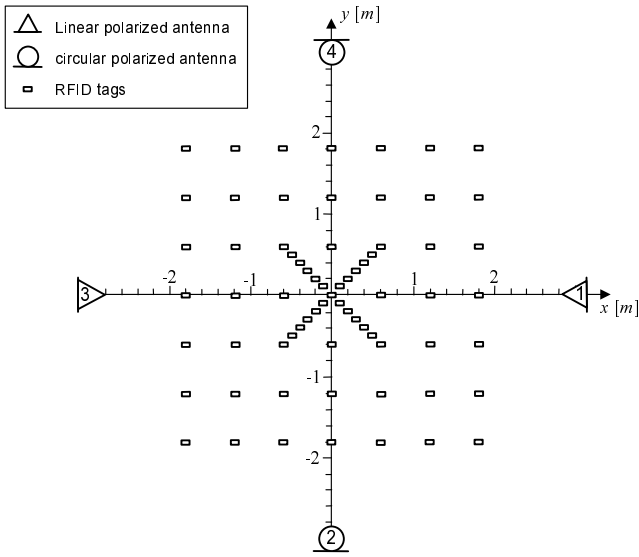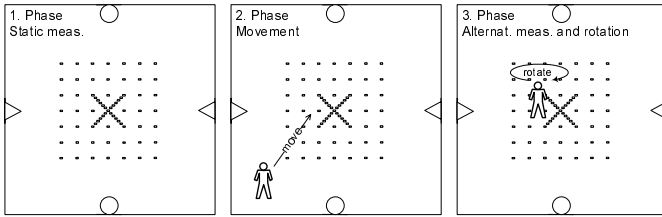
Figure 2. Measurement set-up.

Figure 3. Measurement procedure. The symbols are same as in figure 2.

custom Java program which configured the RFID system, and fetched and stored the measurement data utilizing the provided API.

For the measurements, we choose 6 significant antenna pairs to limit execution time of experiments. Each row of $N_{\mathrm{ap}} \in \mathbb{N}^{6\times 2}$ denotes such a pair whereby the first and the second column indicates the transmitting antenna's and the receiving antenna's identifier, respectively: $N_{\mathrm{ap}} = [[1,2]^T, [1,3]^T, [1,4]^T, [2,3]^T, [2,4]^T, [3,4]^T]^T$ (see Figure 2).

B. Experimental Procedure

The parameters of the measurement series were the location and orientation of a test person. Each measurement comprises three phases:

- 1. Phase: Static measurement of RSS
- 2. Phase: Test person moves to location
- 3. Phase: Alternating static measurements of RSS and rotation of test person.

We investigated 49 different locations (x,y) of the test person whereby at each location 8 different orientations α were tested. The range of parameters was $x,y \in \{-1.8, -1.2, -0.6, \ldots, 1.8\}$ meters and $\alpha \in \{0°, 45°, 90°, \ldots, 315°\}$ respectively, whereby α is the clockwise angle between the direction of view of the test person and the x-axis. The timing and anti-collision parameters of the system were chosen such that on average 10 RSS values
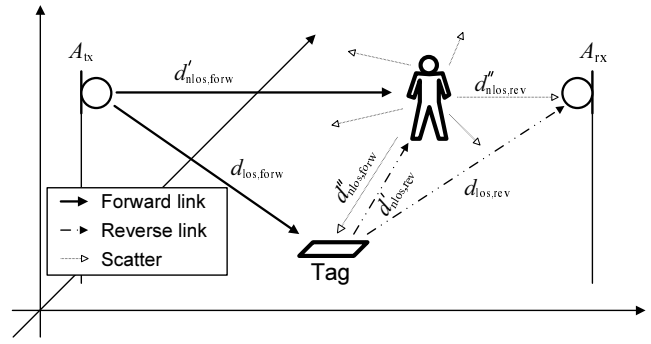

Figure 4. Scatterers contribute to the fluctuations on the reverse link and lead to attenuation and amplification according to the phase difference of different signal components at the receiving antenna.

for each parameter set (location and orientation) could be acquired.

The measurement data was stored on the host computer and analyzed afterwards.

V. CHARACTERIZING THE IMPACT OF HUMAN PRESENCE ON RSS

Next we characterize in more detail the obstacle dependent loss L_{obst} through experimental measurements. The investigations aim at providing experimental results of RSS of test person being at different locations , compared with initial RSS readings without human presence.

Figure 4 depicts a typical situation of the second phase during a measurement. The test person enters the deployment area and acts as scatterer to the ongoing wireless communications. The relative excess path length d_{exc} of the direct line-of-sight (LOS) and the scattered non-line-of-sight (NLOS) path is significant for the change of RSS regarding the initial RSS readings.

$$d_{\mathrm{exc}} = d'_{\mathrm{nlos}} + d''_{\mathrm{nlos}} - d_{\mathrm{los}} \qquad (4)$$

The ratio between excess path length and signal wave length determines whether two interfering signals' amplitudes add or subtract. Lines of equal excess path length form ellipsoids with A_{tx} and A_{tx} as focii. For example the region $d_{\mathrm{exc}}/\lambda \leq 0.25$ is called the *First Fresnel Zone*. Obstacles in the First Fresnel Zone typically result in attenuations of RSS [5].

Before we begin examining the measurements, we first review a theoretical model for the impact of the scatterer on RSS. Typically, available backscatter RFID systems use the ISM frequency bands and usually occupy a bandwidth of several kHz. In such systems, the bandwidth is very small compared to the carrier frequency and thus it is reasonable to approximate signals as pure tone for our investigations. Hence, a typical radio signal can be described by $\underline{A} = A\, e^{j\omega(t-d/c)}$ where c is the propagation speed of the signal, d the distance covered by the signal and $\omega = 2\pi c/\lambda$. Without loss of generality, we assume that the initial phase of the signal equals zero.

The reference signal travels on the direct path to the receiver, hence, at the receiver we have $\underline{A}_{\mathrm{los}} = A_{\mathrm{los}}\, e^{j\omega(t-d_{\mathrm{los}}/c)}$.
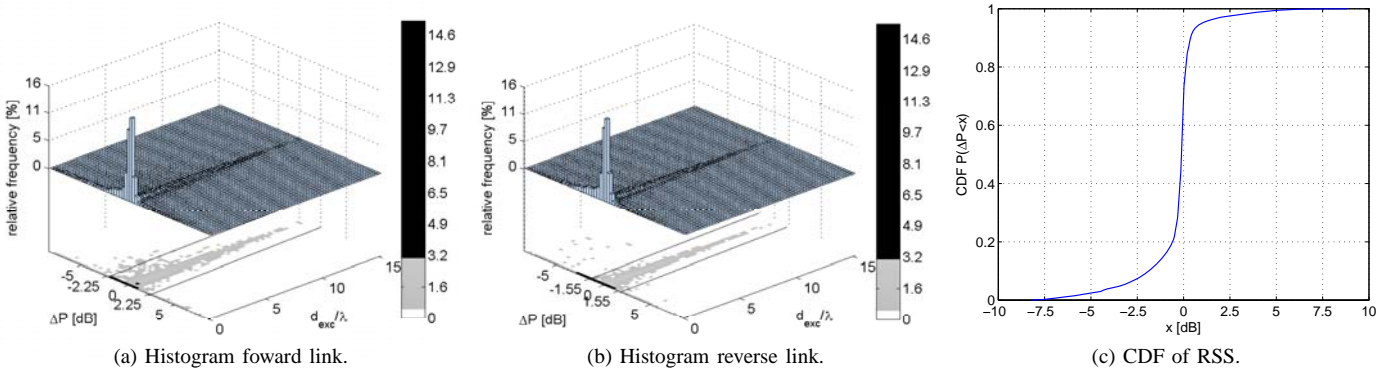
Figure 5. Histogram of measured RSS variations caused by human presence.

(a) Histogram forward link.   (b) Histogram reverse link.   (c) CDF of RSS.

We further assume that an object is present in the vicinity of the line segment between transmitting and receiving antenna that reflects significant part of the energy. Therefore, a second signal with same frequency but different energy $|\underline{A}|^2$ and phase interferes at the receiver $\underline{A}_{\mathrm{nlos}} = A_{\mathrm{nlos}} e^{j\omega(t-(d_{\mathrm{nlos},1}+d_{\mathrm{nlos},2})/c)+j\phi_{\mathrm{refl}}}$.

As a consequence, the signal $\underline{A}$ at the receiving antenna can be formulated as the sum of the two radio waves from the scattering object and from the transmitting antenna:

$$
\begin{aligned}
\underline{A} &= \underline{A}_{\mathrm{los}} + \underline{A}_{\mathrm{nlos}} = Ae^{j(\omega t+\phi)} \\
\mathcal{E} &= |\underline{A}|^2 = \underline{A}\underline{A}^* \\
&= A_{\mathrm{los}}^2 + A_{\mathrm{nlos}}^2 + 2A_{\mathrm{los}}A_{\mathrm{nlos}}\cos\left(kd_{\mathrm{exc}}+\phi_{\mathrm{refl}}\right) \quad (5)
\end{aligned}
$$

Here, $(\cdot)^*$ denotes complex conjugation, ϕ_{refl} the phase shift due to reflection, $\underline{(\cdot)}$ a complex variable and $k = 2\pi/\lambda$. Since the phase of the signal can not be measured by the current system, we leave it unconsidered here.

The amplitude of radio waves dissipates with distance and, therefore, the signal energy at the receiving antenna does not only depend on the excess path length but also on the absolute distances between the antennas and the obstacle. Since we are only interested in characterizing the change of signal energy $\Delta\mathcal{E}$, we reformulate (5) as:

$$
\begin{aligned}
\Delta\mathcal{E} &= \mathcal{E} - |\underline{A}_{\mathrm{los}}|^2 \\
&\approx 2A_{\mathrm{los}}A_{\mathrm{nlos}}\cos\left(kd_{\mathrm{exc}}+\phi_{\mathrm{refl}}\right) \quad A_{\mathrm{los}} \gg A_{\mathrm{nlos}} \quad (6)
\end{aligned}
$$

It is noted that in general there will be more than one excess path. In this case (6) can be reformulated to accommodate for the interference between each pair of impinging signals.

$$
\Delta\mathcal{E} \approx \sum_{j>i}^{M}\sum_{i=1}^{M} 2A_i A_j \cos\left(kd_{\mathrm{exc}}+\phi_{\mathrm{refl}}\right) \quad (7)
$$

Where A_1 denotes the line-of-sight component, M denotes the total number of significant excess paths and $A_1 \gg A_i \ (i > 1)$. We later use (6) to fit the experimental data.

Since the current system provides an indicator of RSS (RSSi) which is proportional to the energy of the impinging signal $\mathcal{E}$, we are able to determine the variation of RSSi
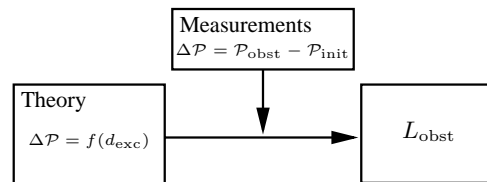

Figure 6. Measurements of received signal strength $\mathcal{P}_{\mathrm{obst}}$, $\mathcal{P}_{\mathrm{init}}$ are used to determine the variation caused by human presence $\Delta\mathcal{P}$ and finally fit the measurements to theory to characterize the obstacle dependent loss L_{obst}.

$\Delta\mathcal{P}$ for different locations of the test person compared to measurements without human presence (see Figure 6).

To facilitate further considerations, we define the following quantities in dB

$\mathcal{P}_{\mathrm{init}}$ is the initial RSSi as measured without human presence in the deployment area.

$\mathcal{P}_{\mathrm{obst}}$ is the RSSi as measured with human presence at a specific location in the deployment area.

$\Delta\mathcal{P}$ denotes the difference or variation of RSSi $\Delta\mathcal{P} = \mathcal{P}_{\mathrm{obst}} - \mathcal{P}_{\mathrm{init}}$.

In the following, we analyse $\Delta\mathcal{P}$ knowing that variation are caused by the presence of the test person and, hence, can be attributed to L_{obst}

A. Analysis of Joint Histogram

In this section we consider the joint histogram $P(\Delta\mathcal{P}; d_{\mathrm{exc}})$ of the excess path length d_{exc} and the variation of received signal strength $\Delta\mathcal{P}$ which is a two-dimensional density function containing the relative number of simultaneous occurrences of the two parameters.

For the calculation of the excess path length d_{exc} we need several quantities (see eq. (4) and Figure 4). However, since the complexity of the humans body prohibits an analytical calculation, we apply a simplified model and regard it as a cylinder of radius 0.15 m and height 1.9 m. This way, the path length of each NLOS line segment in Figure 4 can be determined using simple ray tracing.

It is noted that the variation of RSS can not be attributed specifically to either forward or reverse link since the system
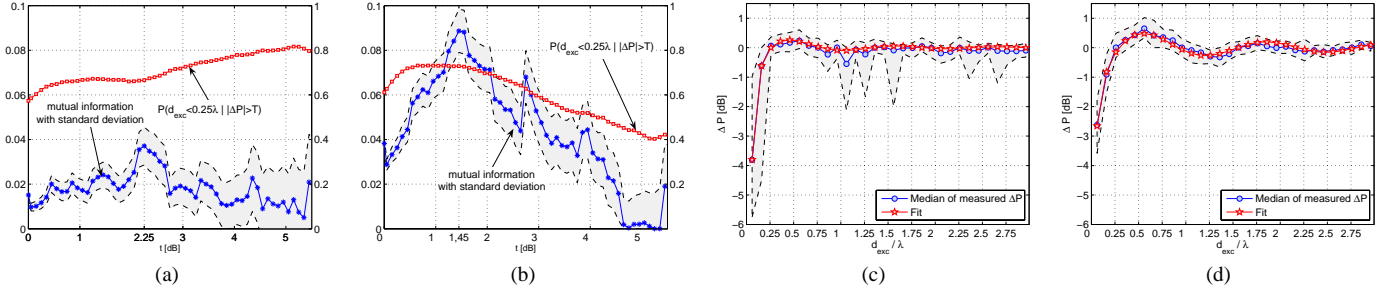
Figure 7. Figures a)–b) depict probability of correct detection and mutual information. Figures c)–d) show the measured relation and the approximation using (9) between d_{exc} and $\Delta\mathcal{P}$. Figures c) and d) depict the results for linear polarized antennas only and averaged over all orientations.

does only allow for measuring the RSS at A_{rx}. However, each RSS measurement is associated with one excess path length for *each* link, forward and reverse. Consequently, the following investigations will distinguish between forward and reverse link through assuming that RSS measurements were caused by the influence of the test person on either link which is reflected by the calculation of d_{exc}. The goal of the following analysis is to determine whether the reverse *or* the forward link excess path lengths explain the RSS variations best. This way, we also gain insight into how reliable we can infer the excess path length from RSS variations which would be the basis for localization algorithms.

Figure 5 (a) and (b) depict $P(\Delta\mathcal{P}; d_{\mathrm{exc}})$ for forward and reverse links, respectively. The difference of the two histograms becomes more visible when considering the shaded plot in the bottom of the two figures. In general, the histogram values concentrate in the region $\{d_{\mathrm{exc}}/\lambda \in (0, 0.5); \Delta\mathcal{P}/dB \in (-3.4, 1)\}$. It is shown that the forward link shows a wider spread of attenuations than the reverse link especially in the region $d_{\mathrm{exc}}/\lambda \leq 5$. In contrast, the histogram of the reverse link shows a more distinct relation between the two parameters. Furthermore, the histogram of the reverse link indicates more frequent and stronger attenuations (black area) than the forward link.

Figures 5 (c) shows the two dimensional marginal histogram of $\Delta\mathcal{P}$. It is shown that human presence causes more attenuation than amplifications since the CDF shows a steeper increase for $\Delta\mathcal{P} \leq -1$ dB than for $\Delta\mathcal{P} \geq 1$ dB. Furthermore, 80 % of measured RSSi are in the range -1 dB $< \Delta\mathcal{P} < 1$ dB. Considering the Figures 5 (a) and (b), we observe that this region has non-zero relative frequencies also for large d_{exc} which makes inferring d_{exc} from $\Delta\mathcal{P}$ difficult.

B. Inferring excess path length from RSS

We now consider the success rate of mapping RSS variations to an excess path length. One way to do this is to use the mutual information $I(\Delta\mathcal{P}; d_{\mathrm{exc}})$ of the joint histogram. The mutual information tells us how much knowing one random variable, i.e. $\Delta\mathcal{P}$, reduces the uncertainty of a second random variable, i.e. d_{exc}. The higher the mutual information the more information is contained in a measurement of RSS about the

excess path length and, therefore, about the location.

$$I(\Delta\mathcal{P}; d_{\mathrm{exc}}) = \sum_{x \in \Delta\mathcal{P}} \sum_{y \in d_{\mathrm{exc}}} P(x, y) \log \frac{P(x, y)}{p(x)p(y)} \quad (8)$$

Whereby $p(\cdot)$ denotes marginal probability. Since measurements are defective, we use a method developed by Moddemeijer to estimate the mutual information [6]. Since the joint histogram is strongly concentrated, we restrict the investigations to mapping $\Delta\mathcal{P}$ to $d_{\mathrm{exc}} < 0.25\lambda$, i.e. the first Fresnel Zone.

Considering the joint histogram, we recognize that small variation of RSS, e.g. $|\Delta\mathcal{P}| < T$, occur for a wide range of excess path length which makes inferring d_{exc} from $\Delta\mathcal{P}$ difficult. Therefore, we apply a threshold T and discard readings with $|\Delta\mathcal{P}| < T$. The question is: What is the optimal value of T regarding inferring d_{exc} from $\Delta\mathcal{P}$?

To answer this question, we consider two metrics. First, the probability of the user being within the first Fresnel Zone given a RSS measurement with $|\Delta\mathcal{P}| > T$ and, second, estimates of the mutual information $I(\Delta\mathcal{P}; d_{\mathrm{exc}})$. These two quantities are depicted in Figures 7 (a)–(b) versus threshold T for forward and reverse links, respectively. The shaded area around the mutual information depicts the standard deviation of estimates.

It is shown that the probability of correctly mapping $\Delta\mathcal{P}$ to an excess path length of $d_{\mathrm{exc}}/\lambda < 0.25$ proceeds differently for forward and reverse links. Concerning forward links, it almost constantly grows, whereas it shows a maximum for reverse links. Consequently, choosing T is subject to a trade off: On the one hand, it must be assured that enough measurements are available to provide a statistically feasible basis which prefers smaller T. On the other hand, the larger T the more reliable we can infer d_{exc} from $\Delta\mathcal{P}$ which maximizes $P(d_{\mathrm{exc}} < 0.25\lambda | |\Delta\mathcal{P}| > T)$.

To find a good trade off, we consider the mutual information $I(\Delta\mathcal{P}; d_{\mathrm{exc}})$. Comparing $I(\Delta\mathcal{P}; d_{\mathrm{exc}})$ for forward and reverse link reveals that the mutual information shows a more distinct behavior for reverse links.

The mutual information is maximized when using thresholds $T_{\mathrm{forw}} = 2.25$ dB and $T_{\mathrm{rev}} = 1.45$ dB for forward and reverse links, respectively. Applying these thresholds reveals that the reverse link contains more than twice the information about d_{exc} compared with the forward link. Also the probabil-

Table I
PARAMETERS OF FITTING THE MEASUREMENTS.

Parameter	Forward link	Reverse link
A	0.025	0.14
B	−1.32	−0.79
$\tilde{\lambda}$	0.37	0.43
Φ_{refl}	3.20	3.25

ity of correct mapping is 0.73 for the reverse link versus 0.67 for the forward link in this case. This indicates that given a specific $\Delta\mathcal{P}$, we can more reliably infer the excess path length of the reverse link than that of the forward link.

The reason these findings is that obstructions and interference on the forward link are more likely to cause the received signal strength to fall below the sensitivity of the tag and, thereby, causing a total loss of connection. As a consequence, the dynamic range of of RSS is cut below a certain level for forward links which can be thought of as quantization reducing the information contained in the associated measurements.

C. Analytical Approximation

In this section, we characterize the empirical relationship between $\Delta\mathcal{P}$ and d_{exc} to equation (5). Figure 7 (c)–(d) depicts the measured RSS $\Delta\mathcal{P}$ versus the excess path length d_{exc} of forward and reverse link for the linearly polarized antennas, respectively. The shaded area denotes the *Interquartile Range* (IQR) which includes the middle 50% of the sorted data and indicates the spread of measurements. We first consider the measurement data denoted by the lines with circular markers. We consider here only the linearly polarized antennas as the circular polarization seems to smooth the effect that we focus on. However, the impact of polarization can not be investigated due to space limitations.

It is shown that comparatively large attenuations and wide IQR can be associated with small d_{exc} on the forward link. However, $\Delta\mathcal{P}$ is relatively constant for growing excess path lengths indicating that small variations of received power at the tag hardly influence RSS measurements at the reader.

In contrast, the reverse link shows a more characteristic relationship between $\Delta\mathcal{P}$ and d_{exc}. Here, the curve shows a damped oscillation which indicates that scatter from farther test persons contribute significantly to the interference. This supports our findings presented in the previous section that the reverse link contains more information about the location.

Next, we consider fitting the measurements to a reformulation of equation (5) with parameters $A, B, \tilde{\lambda}$ and Φ_{refl}:

$$\Delta\tilde{\mathcal{P}}(d_{\mathrm{exc}}) = A d_{\mathrm{exc}}^{B} \cos\left(2\pi \frac{d_{\mathrm{exc}}}{\tilde{\lambda}} + \Phi_{\mathrm{refl}}\right) \qquad (9)$$

As shown in 7 (c)–(d) the fitted curves represent a reasonable approximation to the measurements. Table I list the parameters of the two fits. As illustrated in the table, the values of $\tilde{\lambda}$ agree well with the true wave length $\lambda \approx 0.344$ m and also the phase shift Φ_{refl}

VI. FUTURE WORK

The results presented indicate that with the current system the user location, being the cause of the variations of RSS, can be narrowed down to the First Fresnel Zone of one link. Considering that a typical RFID-system comprises many tags and therefore many links, we suggest to combine RSS readings of different tags to improve localization accuracy. Obviously, such an localization approach depends on many design parameters which we will investigate in the near future.

VII. CONCLUSION

We present and analyze measurements of received signal strength (RSS) conducted in an indoor environment using a passive bistatic RFID-System. The measurement setup consisted of two linearly and two circularly polarized antennas, a RFID-reader and 69 RFID-tags. Parameters of the measurements were the user location and orientation. Recognizing the influence of human presence on RSS, we focused on the variation of RSS and investigated its dependence on the user location.

Analysis of measurements revealed that it is possible to successfully narrow the user location down to the first Fresnel Zone, an ellipsoid area with sender and receiver as its focii, in 73% of measured links. Furthermore, investigations of the mutual information suggest that the reverse link should be emphasized as the associated readings contain more information on the user location compared with the forward link.

An analytical approximation of the relationship between the RSS variations and the excess path delay of the signals scattered by the user is presented. Forward and reverse link show different behavior in this regard. Forward links are mostly subject to attenuations whereas reverse links show a more distinct behavior with periodic zones of amplification and attenuation. This approximation can be a valuable input to localization techniques.

REFERENCES

[1] D. Kim, M. A. Ingram, and W. W. Smith, "Measurements of small-scale fading and path loss for long range rf tags," *IEEE Transactions on Antennas and Propagation*, vol. 51, no. 8, pp. 1740–1749, 2003.

[2] D. Zhang, M. Jian, Q. Chen, and L. Ni, "An rf-based system for tracking transceiver-free objects," in *5th Annual IEEE International Conference on Pervasive Computing and Communications, PerCom 2007*, White Plains, NY, 2006, pp. 135–144.

[3] N. Patwari and P. Agrawal, "Effects of correlated shadowing: Connectivity, localization, and rf tomography," *Information Processing in Sensor Networks, 2008. IPSN '08. International Conference on*, pp. 82–93, April 2008.

[4] P. Nikitin and K. Rao, "Antennas and propagation in uhf rfid systems," in *IEEE International Conference on RFID*, April 2008, pp. 277–288.

[5] W. Lee, *Mobile communications engineering*. McGraw-Hill Professional, 1982.

[6] R. Moddemeijer, "On estimation of entropy and mutual information of continuous distributions," *Signal Processing*, vol. 16, no. 3, pp. 233–246, 1989.